

Level Lines as Global Minimizers of Energy Functionals in Image Segmentation

Charles Kervrann, Mark Hoebeke, and Alain Trubuil

INRA - Biométrie, Domaine de Vilvert
78352 Jouy-en-Josas, France
{ck,mh,at}@jouy.inra.fr

Abstract. We propose a variational framework for determining global minimizers of rough energy functionals used in image segmentation. Segmentation is achieved by minimizing an energy model, which is comprised of two parts: the first part is the interaction between the observed data and the model, the second is a regularity term. The optimal boundaries are the set of curves that globally minimize the energy functional. Our motivation comes from the observation that energy functionals are traditionally complex, for which it is usually difficult to precise global minimizers corresponding to “best” segmentations. Therefore, we focus on basic energy models, which global minimizers can be explicitly determined. In this paper, we prove that the set of curves that minimizes the image moment-based energy functionals is a family of level lines, i.e. the boundaries of level sets (connected components) of the image. For the completeness of the paper, we present a non-iterative algorithm for computing partitions with connected components. It leads to a sound initialization-free algorithm without any hidden parameter to be tuned.

1 Introduction

One of the primary goals of early vision is to segment the domain of an image into regions ideally corresponding to distinct physical objects in the scene. While it has been clear that image segmentation is a critical problem, it has proven difficult to precise segmentation criteria that capture non-local properties of an image and to develop efficient algorithms for computing segmentations. There is a wide range of image segmentation techniques in the literature. Many of them rely on the design and minimization of an energy function which captures the interaction between models and image data [10, 2, 21, 15, 27]. Conventional segmentation techniques generally fall into two distinct classes, being either boundary-based or region-based. The former class looks at the image discontinuities near objects boundaries, while the latter examines the homogeneity of spatially localized features inside objects boundaries. Based on these properties, each of these has characteristic advantages and drawbacks. Nevertheless, several methods combine both approaches [29, 7, 5, 12].

Region-based approaches are our main interest. In contrast to boundary-based methods, region-based approaches try to find partitions of the image pixels into zones the most homogeneous possible corresponding to coherent image

properties such as brightness, color and texture. Homogeneity is traditionally measured by a given global objective function and hard decisions are made only when information from the whole image is examined at the same time. In that case, the boundaries are the set of curves that minimizes a global energy function. Past approaches have centered on formulating the problem as the minimization of a functional involving the image intensity and edge functions. Some energy models are based on a discrete model of the image, such as Markov random fields [10, 15, 27] or a *Minimum Description Length* (MDL) representation [15, 8], whereas variational models are based on a continuous model of the image [2, 21, 20, 19, 26]. More recently, Zhu attempted to unify snakes, region growing and energy/Bayes/MDL within a general framework [29]. Finally, Blake and Zisserman [2] and Mumford and Shah [21] have written about most aspects of this approach to segmentation and have proposed various complex functionals whose minima correspond to segmented images. In a recent review, Morel and Solimini [19] have, indeed, shown that most approaches aim at optimizing a cost functional which is the combination of three terms: one which ensures that the smoothed image approximates the observed one, another which states that the gradient of the smoothed image should be small, except on a discontinuity set, and a last one which ensures that the discontinuity set has a small length. In other respects, while these different approaches offer powerful theoretical frameworks and minimizers exist [19, 29, 26], it is often computationally difficult to minimize the associated functions. Typically, some embedding procedure, like graduate-non-convexity [2], is used to avoid bad local minima of cost functionals. A fairly complete analysis is available only for a simplified version of the Mumford and Shah model that approximates a given image with piecewise constant functions [19]. Moreover, in the area of region-based approaches, layers approaches attempted to use both region and boundary information [8]. But the number of layers and the values associated with the layers must be known *a priori* or estimated using ad-hoc methods or prohibitive Expectation-Maximization procedures.

The main obstacle of energy model based approaches is to find more effective and faster ways of estimating the boundaries and values for regions minimizing the energy than those presently available. This motivates the search for global minimizers of energy functionals commonly used in image segmentation. The key contribution of this paper is to provide basic energy models, which global minimizers can be explicitly determined in advance. Accordingly, energy minimization methods and iterative algorithms are not necessary to solve the optimization problem. The energy model introduced in a discrete setting by Beaulieu and Goldberg [1] and reviewed by Morel and Solimini [19] has been the starting point for our own work. This model tends to obtain a partition with a small number of regions and small variances without *a priori* knowledge on the image. The cost function allows to partition the image into regions, though in a more restrictive manner than previous approaches [21, 2, 15, 29] since it can generate irregular boundaries [19]. In [1], the energy is efficiently minimized using a split-and-merge algorithm. Here, our approach is completely different to determine

global minimizers of similar energy models. The present investigation is based on a variational model. In Section 2, we prove that the set of curves that minimizes a particular class of energy models is a family of level lines defined from level sets of the image. We list some prior models (Markov connected component fields, entropy prior) which are consistent with this theoretical framework. In this sense, the method is deterministic and equivalent to a procedure that selects the “best” level lines delimiting object boundaries. The rest of the paper is organized as follows. A description of the initialization-free segmentation algorithm is included in Section 3. In Section 4, experiments on several examples demonstrate the effectiveness of the approach.

2 The framework

One approach to the segmentation problem has been to try to globally minimize what we call the “energy” of the segmentation. These energy models are usually used in conjunction with Bayes’s theorem. Most of the time, the energy is designed as a combination of several terms, each of them corresponding to a precise property which much be satisfied by the optimal solution. The models have two parts: a *prior model* E_p and a *data model* E_a . The prior term is sometimes called the “regularizer” because it was initially conceived to make the problem of minimizing the data model well-posed.

2.1 Minimization problem

Our theoretical setting is the following. Let us consider a real-value function I , i.e. the image, whose domain is denoted $S : [0, a] \times [0, b]$. In many situations, it is convenient to consider images as real-valued functions of continuous variables. We define the solution to the segmentation problem as the global minimum of a regularized criterion over all regions.

Let $s = (x, y) \in S$ an image pixel, $\Omega_i \subset S$, $i = 1, \dots, P$, an non-empty image domain or object and $\partial\Omega_i$ its boundary. We associate with the unknown domains Ω_i the following regularized objective function, inspired from [1, 11]:

$$\begin{cases} E_\lambda(f, \Omega_1, \dots, \Omega_P) = E_a(f, \Omega_1, \dots, \Omega_P) + \lambda E_p(\Omega_1, \dots, \Omega_P) \\ E_a(f, \Omega_1, \dots, \Omega_P) = \sum_{i=1}^P E_a(f, \Omega_i) \end{cases} \quad (1)$$

where f is any integrable function, for instance the convolution of the image I with any filter, $E_p(\Omega_1, \dots, \Omega_P)$ is a penalty functional and $\lambda > 0$ is the regularization parameter. Some choices of f have been recently listed in [12]. Here, we just consider the possibility of examining the image at various scales using a Gaussian smoothing of the image, including the case of zero variance, i.e. $f = I$ and the case of anisotropic diffusion [14].

Equation (1) is the most general form of energy we can optimize globally at present. We present two appropriate energy models for segmentation which attempt to capture homogeneous regions with unknown constant intensities. It will be clear that none of these models captures all the important scene variables but may be useful to provide a rough analysis of the scene.

LEAST SQUARES CRITERION: In this modeling, implicitly, a Gaussian distribution for the noise is assumed [19, 29]. The data model is usually defined as

$$E_a(f, \Omega_1, \dots, \Omega_P) = \sum_{i=1}^P \int_{\Omega_i} (f(x, y) - \bar{f}_{\Omega_i})^2 dx dy \quad (2)$$

where \bar{f}_{Ω_i} denotes the average of f over Ω_i . This means that one observes a corrupted function $f = f_{\text{true}} + \varepsilon$, where ε is a zero-mean Gaussian white noise and f_{true} is supposed piecewise constant, i.e.

$$f_{\text{true}}(s) = \sum_{i=1}^P \bar{f}_{\Omega_i} \mathcal{I}(s \in \Omega_i) \quad \text{where} \quad |\Omega_i| = \int_{\Omega_i} dx dy, \quad (3)$$

and $\mathcal{I}(\cdot)$ is the indicator function. The standard deviation is assumed to be constant over the entire image. The image domain S is split into unknown P disjoint regions $\Omega_1, \dots, \Omega_P$.

CONTRAST STATISTIC CRITERION: One may be interested in identifying boundaries corresponding to sharp contrast in the image. We define the contrast of a boundary by the difference between the average value of f per unit area on the inside of the boundary and the outside of the object, that is the background Ω_P [23]. Formally, the corresponding data model is

$$E_a(f, \Omega_1, \dots, \Omega_P) = - \sum_{i=1}^{P-1} (\bar{f}_{\Omega_i} - \bar{f}_{\Omega_P})^2. \quad (4)$$

Regions are assumed to be simple closed curves superimposed on the background. This data model does appear to have a fairly wide application potential, especially in medical image analysis and confocal microscopy, where the regions of interest appear as bright objects relative to the dark background.

For the sake of clarity, we restrict ourselves to the first case, i.e. the **LEAST SQUARES CRITERION**, and give major results for the other criterion.

Our aim is now to define objects in f . Therefore, we define the following class C_P , $P \geq 1$ of admissible objects

$$C_P = \{(\Omega_1, \dots, \Omega_{P-1}) \subset S \text{ are regular, closed and connected ; } \cup_{i=1}^P \Omega_i = S ; \\ 1 \leq i, j \leq P, i \neq j \implies \Omega_i \cap \Omega_j = \emptyset ; \}$$

where the subsets $(\Omega_1, \dots, \Omega_{P-1})$ are the objects of the image and Ω_P is the background. When $P = 1$, there is no object in the image. An optimal segmentation of image f over C_P is by definition a global minimum of the energy (when exists)

$$(\Omega_1^*, \dots, \Omega_{P^*}^*) = \inf_{P \geq 1} \inf_{(\Omega_1, \dots, \Omega_P) \in C_P} E_\lambda(f, \Omega_1, \dots, \Omega_P). \quad (5)$$

A direct minimization with respect to all unknown domains Ω_i and parameters \bar{f}_{Ω_i} is a very intricate problem [2, 21, 19, 29]. In the next section, we prove that the object boundaries are level lines of function f if the penalty function E_p only encourages the emergence of a small number of regions. In our context, an entropy prior or Markov connected component fields-based prior are used to reduce the number of regions. The parameter λ can be then interpreted as a scale parameter that only tunes the number of regions [19].

2.2 Minimizer description and level lines

Our estimator is defined by (when exists)

$$(\hat{\Omega}_1, \dots, \hat{\Omega}_{\hat{P}}) = \operatorname{argmin}_{P \geq 1} \operatorname{argmin}_{(\Omega_1, \dots, \Omega_P) \in C_P} E_\lambda(f, \Omega_1, \dots, \Omega_P). \quad (6)$$

The question of the existence of an admissible global minimum for energies like Mumford and Shah's energy [21] is a difficult problem (see [19] for more details). Here, our aim is not to investigate conditions for having an admissible global minimum. In what follows, we make an *ad-hoc* assumption ensuring the existence of a unique minimum of the energy [11].

Minimizer description. We propose the following lemma

LEMMA 1 *If there exists a unique admissible global minimum and that no pathological minimum exists [11], then the set of curves that globally minimizes the energy is a subset of level lines of f :*

$$f|_{\partial\Omega_i} \equiv \mu_i, \quad i = 1, \dots, \hat{P} - 1.$$

i.e. the border $\partial\Omega_i$ of each Ω_i is a boundary of a level set of f .

Proof of Lemma 1 Without loss of generality, we prove Lemma 1 for one object Ω and a background Ω^c , where Ω^c denotes the closure of the complementary set of Ω . For two sets A and B , denote $\int_{A-B} f \triangleq \int_A f - \int_B f$. Let Ω_δ be a small perturbation of Ω , i.e. the Hausdorff distance $d_\infty(\Omega_\delta, \Omega) \leq \delta$. Then, we have

$$\int_{\Omega_\delta - \Omega} \mathbb{1} = \underbrace{|\Omega_\delta| - |\Omega|}_{\Delta(|\Omega|)} \quad \text{and} \quad \left(\int_{\Omega_\delta} f \right)^2 - \left(\int_{\Omega} f \right)^2 = 2 \int_{\Omega} f \int_{\Omega_\delta - \Omega} f + \left(\int_{\Omega_\delta - \Omega} f \right)^2 \quad (7)$$

and the following image moments:

$$m_0 = \int_{\Omega} \mathbb{1}, \quad m_1 = \int_{\Omega} f, \quad m_2 = \int_{\Omega} f^2, \quad K_0 = \int_S \mathbb{1}, \quad K_1 = \int_S f, \quad K_2 = \int_S f^2. \quad (8)$$

The difference between the involved energies is equal to

$$\underbrace{E_\lambda(f, \Omega_\delta, \Omega_\delta^c) - E_\lambda(f, \Omega, \Omega^c)}_{\Delta E_\lambda(f, \Omega, \Omega^c)} = \underbrace{E_d(f, \Omega_\delta, \Omega_\delta^c) - E_d(f, \Omega, \Omega^c)}_{\Delta E_d(f, \Omega, \Omega^c)} + \lambda \underbrace{E_p(\Omega_\delta, \Omega_\delta^c) - E_p(\Omega, \Omega^c)}_{\Delta E_p(\Omega, \Omega^c)}. \quad (9)$$

Table 1. Coefficients A_0 and A_1 associated to the two segmentation criteria.

	A_0	A_1
LEAST SQUARE CRITERION	$\frac{m_1^2}{m_0^2} - \frac{(K_1 - m_1)^2}{(K_0 - m_0)^2}$	$-\frac{2m_1}{m_0} + \frac{2(K_1 - m_1)}{K_0 - m_0}$
CONTRAST STATISTIC CRITERION	$\frac{2m_1^2}{m_0^2} - \frac{2(K_1 - m_1)^2}{(K_0 - m_0)^3}$ $-\frac{2m_1(1 - 2m_0)(K_1 + m_1)}{m_0^2(K_0 - m_0)^2}$	$-\frac{2m_1}{m_0} + \frac{2(K_1 - m_1)^2}{(K_0 - m_0)^2}$ $+\frac{2(K_1 - 2m_1)}{m_0(K_0 - m_0)}$

In Appendix, it is shown that for $\Delta(|\Omega|) \rightarrow 0$, $\Delta E_a(f, \Omega, \Omega^c)$ is equal to

$$\Delta E_a(f, \Omega, \Omega^c) = \Delta(|\Omega|) (A_0 + A_1 f) + O(\Delta(|\Omega|)^2) \quad (10)$$

where A_0 and A_1 are computed from image moments given in (8). For the two criteria described in Section 2.1, the coefficients are listed in table 1. Suppose we can write $\Delta E_p(\Omega, \Omega^c)$ as

$$\Delta E_p(\Omega, \Omega^c) = \Delta(|\Omega|) (B_0 + B_1 f) + O(\Delta(|\Omega|)^2). \quad (11)$$

Let s_0 be a fixed point of the border $\partial\Omega$. Choose Ω_δ such that $\partial\Omega_\delta = \partial\Omega$ except on a small neighborhood of s_0 . The energy having a minimum for Ω , $f(s_0)$ needs to be solution of the following equation

$$\Delta E_\lambda(f, \Omega, \Omega^c) = \Delta(|\Omega|) [(A_0 + \lambda B_0) + (A_1 + \lambda B_1)f(s_0)] + O(\Delta(|\Omega|)^2) = 0. \quad (12)$$

By pre-multiplying (12) by $\Delta(|\Omega|)^{-1}$ and passing to the limit $\Delta(|\Omega|) \rightarrow 0$, we obtain

$$(A_0 + \lambda B_0) + (A_1 + \lambda B_1)f(s_0) = 0. \quad (13)$$

Equation (13) has an unique solution. The coefficients $(A_0 + \lambda B_0)$ and $(A_1 + \lambda B_1)$ do depend on neither s_0 nor $f(s_0)$, and $A_0 + \lambda B_0 \neq 0$. The function f is continuous and $\partial\Omega$ is a connected curve. Therefore $f(s_0)$ is constant when s_0 covers $\partial\Omega$. \square

In conclusion, we proved that the global minimizer is a subset of iso-intensity curves of the image provided that $E_\lambda(f, \Omega_1, \dots, \Omega_P)$ is explained by second-order image moments. In the next section, we list two penalty functionals relying on the Markov connected component fields and entropy theories, which are consistent with Lemma 1 and (11).

Image representation by level sets. In consequence of Lemma 1, object borders can be determined by boundaries of level sets. Meanwhile, it turns out that the basic information of an image (or function f) is contained in the family of its binary shadows or *level sets*, that is, in the family of sets \mathcal{S}_η defined by

$$\mathcal{S}_\eta = \{s \in S : f(s) \geq \eta\} \quad (14)$$

for all values of η in the range of f [16]. In contrast to edge representation, the family of level sets is a complete representation of f [18]. This representation is invariant with respect to any increasing contrast change and so robust to illumination conditions changes. In general, the threshold set is made up of connected components based both on the image gray levels and spatial relations between pixels. To extract a connected component of a level set \mathcal{S}_η , we threshold the image at the gray level η and extract the components of the binary image we obtain. A more efficient technique has been described in [18]. A recent variant of this representation is proposed in [3, 18] by considering the boundary of level sets, that is the *level lines*. This representation does not differ with respect to the set of level sets. As a consequence of the inclusion property of level sets, the level lines do not cross each other's. In the following, we basically consider that a connected component is an object Ω_i and the level lines are just a set of η -isovalue pixels at the borders $\partial\Omega_i$ of connected components.

2.3 Forms of prior models

One of the difficulties in the Bayesian approach is to assign the prior law to reflect our prior knowledge about the solution. Besides, in consequence of Lemma 1, the set of penalty functionals is limited. The contribution of a given pixel to the prior does not depend on the relation with neighbors and the resulting regions may have noisy boundaries. Here, the proposed penalty functionals are not necessary convex but only enable to select the right number of regions. Instead of fixing *a priori* the cardinality of the segmentation, which is a highly arbitrary choice, it seems more natural to control the emergence of regions by an object area-based penalty or by an information criterion weighted by a scale parameter λ .

Markov connected component fields. A new class of Gibbsian models with potentials associated to the connected components or homogeneous parts has been introduced in [17]. For these models, the neighborhood of a pixel is not fixed as for Markov random fields, but given by the components which are adjacent to the pixel. These models are especially applicable for images where a relatively few number of gray levels occur, and where some prior knowledge is available about size and shape characteristics for the connected components [27]. The Markov connected component fields possess certain appealing Markov properties which have been established in [17].

Here we considered a Markov connected component field which the probability density function is proportional to

$$\exp \underbrace{\sum_{i=1}^{P-1} \alpha |\Omega_i| + \beta (P-1)^{\zeta-1} + \gamma |\Omega_i|^2}_{E_p(\Omega_1, \dots, \Omega_P)}. \quad (15)$$

The parameter γ controls the size of the components since the squared area of the union of two components is greater than the sum of the squared areas of

each component. The size of the components is however also influenced by the parameter α together with the parameters β and ζ which controls the number of components. The potential $E_p(\Omega_1, \dots, \Omega_P)$ is the more general functional we can use since the boundaries of connected components cannot be penalized in our framework. These potentials can be separately used to select the right number of regions by setting $\alpha, \beta, \gamma = \{0, 1\}$.

In Section 2.2, we proved Lemma 1 for one object Ω and a background Ω^c . Using the same notations, we easily write

$$\Delta E_p(\Omega, \Omega^c) = \alpha \Delta(|\Omega|) + \gamma (|\Omega_\delta|^2 - |\Omega|^2) = \Delta(|\Omega|) (\alpha + 2\gamma m_0) + \gamma \Delta(|\Omega|)^2. \quad (16)$$

Accordingly, we obtain $B_0 = (\alpha + 2\gamma m_0)$ and $B_1 = 0$, which is consistent with Lemma 1 and (11) if no pathological events (e.g. topological changes) occurs.

The application of Markov connected component fields is somewhat more computationally demanding than the application of Markov random fields. By the local Markov property the calculations for an update of a site in a single site updating algorithm only involves the components adjacent to this site. Our work may be regarded as an preliminary exploitation of the theoretical framework described by Møller *et al* [17] in image segmentation.

Entropy prior. The entropy function has been widely used as a prior in a Bayesian context for image restoration. Here, the entropy of the segmented image is written as follows [9]

$$E_p(\Omega_1, \dots, \Omega_P) = - \sum_{i=1}^P p_i \ln p_i = - \sum_{i=1}^P \frac{|\Omega_i|}{|S|} \ln \frac{|\Omega_i|}{|S|} \quad (17)$$

where the p_i s represent the histogram values, $|\Omega_i|$ the cardinality of region Ω_i and $|S|$ the cardinality of the image domain. The value p_i is the number of occurrence of the gray level value \bar{f}_{Ω_i} in the segmented image. The histogram entropy is minimized for a Dirac distribution corresponding to one single class in the segmented image. In image segmentation, we want to obtain a histogram sharper than the histogram of the initial image, so the entropy should be minimized [9]. The actual reduction of number of classes is obtained from the information prior $E_p(\Omega_1, \dots, \Omega_P)$. Using the notations introduced in Section 2.2, we write

$$\Delta E_p(\Omega, \Omega^c) = \frac{\Delta(|\Omega|)}{|S|} \ln \frac{|S| - |\Omega|}{|\Omega|} + O(\Delta(|\Omega|)^2). \quad (18)$$

Accordingly, we obtain $B_0 = \frac{1}{|S|} \ln \frac{|S| - |\Omega|}{|\Omega|}$ and $B_1 = 0$, which is consistent with Lemma 1 and (11).

2.4 Properties of the energy models

In this section, we complete the analysis of energy models and discuss the connections with image partitioning algorithms.

Upper bound of the objects number. It appears, most of the time, that variations in the values of the parameters λ have significant effects on the qualitative properties of the minimizer [28]. We show that the maximum number of objects is explicitly influenced by λ .

LEMMA 2 *If there exists an optimal segmentation defined by (1) and (2) then the optimal number P^* of objects is upper bounded by*

$$P_{\max} = 1 + (\lambda |\Omega_{\min}|)^{-1} \int_S (f(x, y) - \bar{f}_S)^2 dx dy$$

$$\text{if } E_P(\Omega_1, \dots, \Omega_P) = \sum_{i=1}^{P-1} |\Omega_i|, \quad \text{i.e. } \alpha = 1, \beta = \gamma = 0.$$

Proof of Lemma 2 :

$$\lambda \sum_{i=1}^{P^*-1} |\Omega_i^*| \leq E_\lambda(f, \Omega_1^*, \dots, \Omega_{P^*}^*) \leq E_\lambda(f, S) = \int_S (f(x, y) - \bar{f}_S)^2 dx dy.$$

If $|\Omega_i| \geq |\Omega_{\min}|$, we have $(P^* - 1)|\Omega_{\min}| \leq \sum_{i=1}^{P^*-1} |\Omega_i^*| \leq \lambda^{-1} \int_S (f(x, y) - \bar{f}_S)^2 dx dy$

and $P^* \leq 1 + (\lambda |\Omega_{\min}|)^{-1} \int_S (f(x, y) - \bar{f}_S)^2 dx dy \quad \square$

Connection to snakes and geodesic active contour models. Let $v_i(s) = (x_i(s), y_i(s))$ denote a point on the common boundary $\partial\Omega_i$ (parametrized by $s \in [0, 1]$) of a region Ω_i and the background Ω_P . We suppose

$$E_\lambda(\Omega_1, \dots, \Omega_P) = \sum_{i=1}^P \int_{\Omega_i} (f(x, y) - \bar{f}_{\Omega_i})^2 dx dy + \lambda \sum_{i=1}^{P-1} |\Omega_i|.$$

The time t dependent position of the boundary $\partial\Omega_i$ can be expressed parametrically by $v_i(s, t)$. The motion of the boundary $\partial\Omega_i$ is governed by the Euler-Lagrange differential equation [29]. For any point $v_i(s, t)$ on the boundary $\partial\Omega_i$ we obtain:

$$\frac{dv_i(s, t)}{dt} = - \frac{\delta E_\lambda(f, \Omega_i, \Omega_P)}{\delta v_i(s)} = [(f(x, y) - \bar{f}_{\Omega_i})^2 + \lambda - (f(x, y) - \bar{f}_{\Omega_P})^2] \mathbf{n}(v_i(s)) \quad (19)$$

where $\mathbf{n}(v_i(s))$ is the unit normal to $\partial\Omega_i$ at point $v_i(s, t)$. This equation can be seen as a degenerate case of the *region competition* algorithm described by Zhu *et al.* [29] where λ is analogous to a pressure term [13, 6]. The solving of the Euler-Lagrange equations for each region can be complex and the *region competition* algorithm (see [29]) finds a local minima. Using the level-set formulation [22, 4, 24], suitable numerical schemes have been derived for solving propagating equations. However, in both cases, seed regions must be provided by the user or randomly put across the image, and mean values \bar{f}_{Ω_i} are updated at each step of the iterative algorithm. In this paper, we directly determined the steady solutions associated with the motion equation given in (19).

3 Segmentation algorithm

In practical imaging, both the domain S and the range of f are discrete sets. The segmentation algorithm we propose is automatic and does not require either the number of regions nor any initial value for regions. This algorithm is not a region growing algorithm as described in [25, 1, 19] since all objects are built once and for all according to (14). Energy minimization is performed once all admissible objects have been registered. To implement our level set image segmentation, a four step method is used.

LEVEL SET CONSTRUCTION The first step completes a crude mapping of each image pixel on a given level set. At present, we uniformly quantize the function $f \in [f_{min}, f_{max}]$ in $K = \{4, 8, 16, 32\}$ equal-sized and non-overlapping intervals $\{[l_1, h_1[, \dots, [l_K, h_K]\}$. Given this set of levels, we then assign one of the levels to each pixel s : s is assigned to $[l_j, h_j[$ if $l_j \leq f(s) < h_j$.

OBJECT EXTRACTION A crude way to build pixels sets corresponding to objects is to proceed to a connected components labeling and to associate each label with an object Ω_i . The background Ω_P corresponds to the complementary set of objects Ω_i . The list of connected components of each of these then forms the list of objects $\{\Omega_1, \dots, \Omega_T\}$ where T is the maximum number of connected components such as $|\Omega_i| \geq |\Omega_{min}|$ and $P \leq T \leq P_{max}$.

Though this process may work in the noise-free case, in general we would also need some smoothing effect of the connected components labeling. So we consider a size-oriented morphological operator acting on sets that consists in keeping all connected components of the output of area larger than a limit Ω_{min} .

CONFIGURATION DETERMINATION The connected components are then combined during the third step to form objects configurations. Having the objects list $\{\Omega_1, \dots, \Omega_T\}$, configurations can be built by enumeration of all possible object combinations, i.e. 2^T configurations. Each possible configuration can then be represented by a binary number b_i which is the binary expansion of i ($0 \leq i \leq 2^T - 1$). The binary value of each bit in b_i determines the presence or absence of a given object in the configuration.

ENERGY COMPUTATION Each configuration represents a set of objects which in turn is a set of pixels. Energy calculations take the image intensities of the original (not quantized) image at each of these pixels to establish mean and approximation error. Note that energies corresponding to each object are computed once and stored, and energy corresponding to the background is efficiently updated for each configuration. The configuration that globally minimizes the energy functional corresponds to the optimal segmentation. The time necessary to perform image segmentation essentially depends on the length of the object list, i.e. the number T of connected components. Nevertheless, all configurations are independent and could be potentially evaluated on suitable parallel architectures.

4 Experimental results

We are interested in the use of the technique in the context of medical and aerial imagery and confocal microscopy. Our system successfully segmented various images into a few regions. For the bulk of the experiments, we used a slightly restricted form, in which the data model is given by (2) and, for the sake of clarity, we restrict ourselves to use a single potential at one and the same time, i.e. $E_p(\Omega_1, \dots, \Omega_P) = P - 1$ or $E_p(\Omega_1, \dots, \Omega_P) = \sum_{i=1}^{P-1} |\Omega_i|$. The last prior model can be re-defined to find large regions with low/high intensity in the image (see Figs. 2-3). Similar results were obtained using an entropy prior. The algorithm parameters were set as follows: $K = 4, 8, 16$ or 32 , and regions which areas $|\Omega_i| < 0.01 \times |S|$ are discarded. Most segmentations took approximately about 4-10 seconds on a 296MHz workstation. Two sets of simulations were conducted on synthetic as well as real-world images to evaluate the performance of the algorithm. In experiments, the image intensities have been normalized into the range $[0, 1]$.

Figure 1a shows an artificially computed 256×256 image representing the superposition of two bidimensional Gaussian functions located respectively at $s_0 = (64, 128)$ and $s_1 = (160, 128)$ with variance of $\sigma_0 = 792$ and $\sigma_1 = 1024$. Figure 1b shows the result of the uniform quantization operation applied on Fig. 1a ($K = 32$). The levels lines associated with the quantized image are displayed on Fig. 1c. Note that level sets of area too small are suppressed. Figures 1d-f show how the penalization parameter influences the segmentation results when $E_p(\Omega_1, \dots, \Omega_P) = \sum_{i=1}^{P-1} |\Omega_i|$. The white borders denote the boundaries of the objects resulting from the segmentation.

We have applied the same algorithm to an aerial 256×256 image depicting the region of Saint-Louis during the rising of the Mississippi and Missouri rivers in July 1993 (Fig. 2a). We are interested in extracting dark regions labelled using \bar{f}_{Ω_i} in this image. The level lines corresponding to $K = 8$ are shown on Fig. 2b. The approach has successfully extracted significant dark regions and labeled in "white" urban areas, forests and fields as "background" (Fig. 2c).

An example in 2D medical imaging is shown on Fig. 3. Figure 3c shows the results of the above method when applied to outline the endocardium of a heart image obtained using Magnetic Resonance. This figure illustrates how our method selects the number of segments in a 2D medical MR image (179×175 image). The level lines are shown in Fig. 3b and the region of interest is successfully located using $K = 8$ and $\lambda = 0.01$.

Confocal systems offer the chance to image thick biological tissue in 2D+t or 3D dimensions. They operate in the bright-field and fluorescence modes, allowing the formation of high-resolution images with a depth of focus sufficiently small that all the detail which is imaged appears in focus and the out-of-focus information is rejected. Some of the current applications in biological studies are in neuron research. We have tested the proposed algorithm on 2D confocal microscopy 256×240 images (Fig. 4a), courtesy of INSERM 413 IFRMP n°23 (Rouen, France). Figure 4a depicts a triangular cell named "astrocyte". These cells generally take the place of died neuron cells. In Figs.4b-c, the seg-

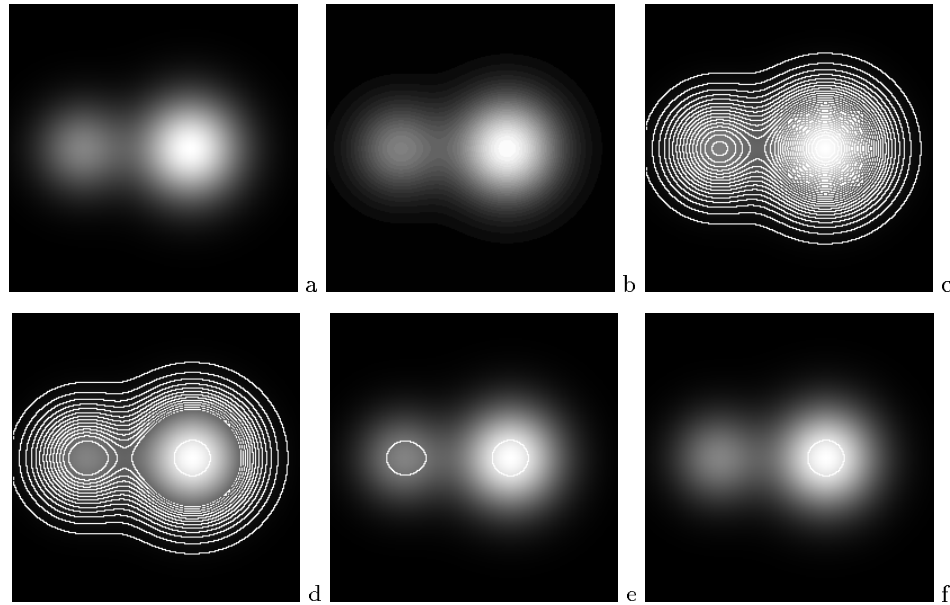


Fig. 1. Segmentation results of a synthetic image. a) original image ; b) uniformly quantized image ($K = 32$) ; c) level lines superimposed on the quantized image ; d) segmentation with $\lambda = 0.01$; e) segmentation with $\lambda = 0.1$ – two detected objects; f) segmentation with $\lambda = 1.0$ – one detected object.

mentation of one single cell is shown. We have preliminary filtered the image using anisotropic diffusion [14]. The boundaries of the cell components are quite accurately delineated in Fig. 4b ($K = 8$, $\lambda = 0.001$).

5 Conclusion and perspectives

In this paper we have proposed basic energy functionals for the segmentation of regions in images, and we proved that the minimizer of our energy models can be explicitly determined. The minimization requires no initialization, and is highly parallelizable. A total CPU time of a few seconds for segmenting a 256×256 image on a workstation makes the method attractive for many time-critical applications. The contribution of this approach has been illustrated on synthetic as well as real-world images. The energies are of a very general form and always globally optimizable by the same algorithm. The framework offers many other possibilities for further modeling. We are currently studying an adaptive quantization technique instead of the uniform quantization used at present to estimate the objects. Finally, the extension of the approach to volumetric images (confocal microscopy) and multi-spectral images is also of interest. In this setting, the structure of the algorithm would be largely the same, although there are a number of points which would need to be examined closely.

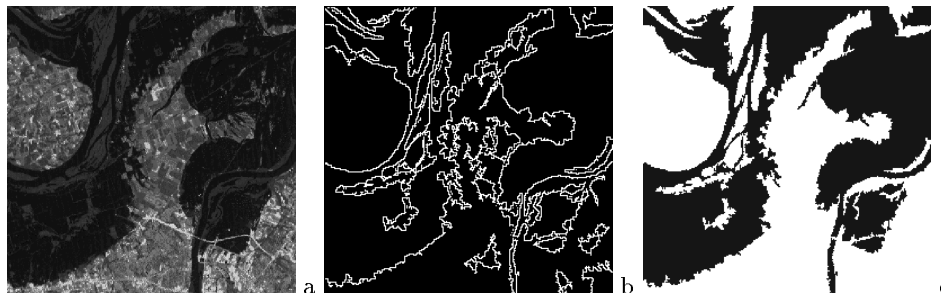


Fig. 2. Segmentation results of an aerial image ($\lambda = 0.001$). Left: original image. Middle: level lines computed from the quantized image ($K = 8$). Right: label map.

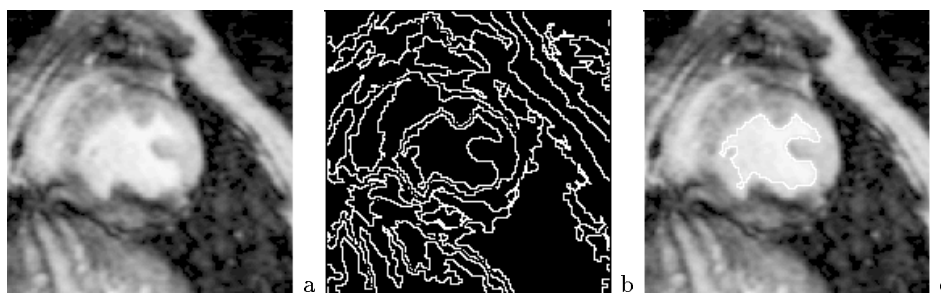


Fig. 3. Segmentation results of a MR image ($\lambda = 0.01$). Left: original image. Middle: level lines computed from the quantized image ($K = 8$). Right: boundaries of the object of interest superimposed on the original image.

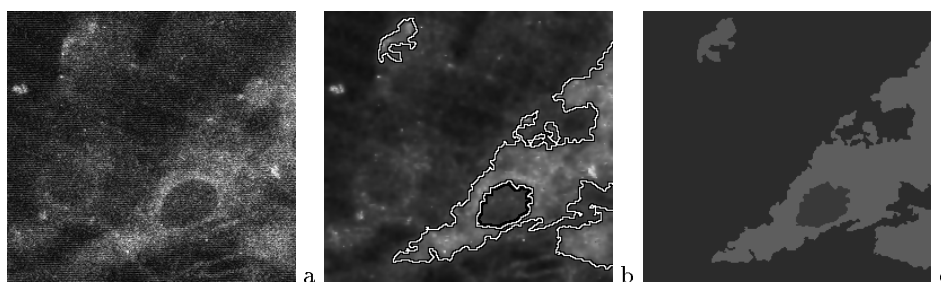


Fig. 4. Segmentation in 2D confocal microscopy ($\lambda = 0.001$). Left: original image. Middle: boundaries superimposed on a adaptively filtered image ($K = 8$). Right: label map.

A Computation of the energy variation for the LEAST SQUARES CRITERION

We compute the energy variation for one object Ω and a background Ω^c , where Ω^c denotes the closure of the complementary set of Ω . The data model is

$$E_a(f, \Omega, \Omega^c) = \int_{\Omega} (f(x, y) - \overline{f_{\Omega}})^2 dx dy + \int_{\Omega^c} (f(x, y) - \overline{f_{\Omega^c}})^2 dx dy. \quad (20)$$

For two sets A and B , denote $\int_{A-B} f \triangleq \int_A f - \int_B f$. Let Ω_{δ} be a small perturbation of Ω , i.e. the Hausdorff distance $d_{\infty}(\Omega_{\delta}, \Omega) \leq \delta$. Then, we define

$$\int_{\Omega_{\delta}-\Omega} \mathbb{I} = \underbrace{|\Omega_{\delta}| - |\Omega|}_{\Delta(|\Omega|)} \quad \text{and} \quad \left(\int_{\Omega_{\delta}} f \right)^2 - \left(\int_{\Omega} f \right)^2 = 2 \int_{\Omega} f \int_{\Omega_{\delta}-\Omega} f + \left(\int_{\Omega_{\delta}-\Omega} f \right)^2. \quad (21)$$

The difference between the involved energies is equal to $\Delta E_a(f, \Omega, \Omega^c) = E_a(f, \Omega_{\delta}, \Omega_{\delta}^c) - E_a(f, \Omega, \Omega^c) = T_1 + T_2 + T_3 + T_4$, with

$$\begin{aligned} T_1 &= \int_{\Omega_{\delta}} f^2 - \int_{\Omega} f^2, & T_2 &= -\frac{1}{|\Omega_{\delta}|} \left(\int_{\Omega_{\delta}} f \right)^2 + \frac{1}{|\Omega|} \left(\int_{\Omega} f \right)^2, \\ T_3 &= \int_{S-\Omega_{\delta}} f^2 - \int_{S-\Omega} f^2, & T_4 &= -\frac{1}{|S| - |\Omega_{\delta}|} \left(\int_{S-\Omega_{\delta}} f \right)^2 + \frac{1}{|S| - |\Omega|} \left(\int_{S-\Omega} f \right)^2. \end{aligned}$$

Using (21) and passing to the limit $\Delta(|\Omega|) \rightarrow 0$, i.e. $|\Omega_{\delta}| \simeq |\Omega|$, we obtain (higher order terms are neglected)

$$\begin{aligned} T_1 &= -T_3 = \int_{\Omega_{\delta}-\Omega} f^2, \\ T_2 &= -\frac{2}{|\Omega|} \int_{\Omega_{\delta}-\Omega} f \int_{\Omega} f - \frac{1}{|\Omega|} \left(\int_{\Omega_{\delta}-\Omega} f \right)^2 + \frac{1}{|\Omega|^2} \int_{\Omega_{\delta}-\Omega} \mathbb{I} \left(\int_{\Omega} f \right)^2, \\ T_4 &= \frac{2}{|S| - |\Omega|} \int_{\Omega_{\delta}-\Omega} f \int_{S-\Omega} f - \frac{1}{|S| - |\Omega|} \left(\int_{\Omega_{\delta}-\Omega} f \right)^2 \\ &\quad - \frac{1}{(|S| - |\Omega|)^2} \int_{\Omega_{\delta}-\Omega} \mathbb{I} \left(\int_{S-\Omega} f \right)^2. \end{aligned} \quad (22)$$

Define the image moments $m_0 = \int_{\Omega} \mathbb{I}$, $m_1 = \int_{\Omega} f$, $K_0 = \int_S \mathbb{I}$, $K_1 = \int_S f$.

Using the *mean value theorem for double integral*, which states that if f is continuous and A is bounded by a simple curve, then for some point s_0 in A we have $\int_A f(s) dA = f(s_0) \cdot |A|$ where $|A|$ denotes the area of S , it follows that

$$\begin{aligned} \Delta E_a(f, \Omega, \Omega^c) &= \overbrace{\left[\frac{m_1^2}{m_0^2} - \frac{(K_1 - m_1)^2}{(K_0 - m_0)^2} \right]}^{A_0} \int_{\Omega_{\delta}-\Omega} \mathbb{I} + \overbrace{\left[-\frac{2m_1}{m_0} + \frac{2(K_1 - m_1)}{K_0 - m_0} \right]}^{A_1} f(s_0) \int_{\Omega_{\delta}-\Omega} \mathbb{I} \\ &\quad - \left[\frac{1}{m_0} + \frac{1}{K_0 - m_0} \right] f(s_0)^2 \left(\int_{\Omega_{\delta}-\Omega} \mathbb{I} \right)^2. \end{aligned} \quad (23)$$

References

1. J. Beaulieu and M. Goldberg. Hierarchy in picture segmentation: a stepwise optimization approach. *IEEE Trans. Patt. Anal. and Mach. Int.*, 11(2):150–163, 1989.
2. A. Blake and A. Zisserman. *Visual Reconstruction*. MIT Press, Cambridge, Mass, 1987.
3. V. Caselles, B. Coll, and J. Morel. Topographic maps. *preprint CEREMADE*, 1997.
4. V. Caselles, R. Kimmel, and G. Sapiro. Geodesic active contours. *Int J. Computer Vision*, 22(1):61–79, 1997.
5. A. Chakraborty and J. Duncan. Game-theoretic integration for image segmentation. *IEEE Trans. Patt. Anal. and Mach. Int.*, 21(1):12–30, 1999.
6. L. Cohen. On active contour models and balloons. *CVGIP: Image Understanding*, 53(2):211–218, 1991.
7. L. Cohen. Deformable curves and surfaces in image analysis. In *Int. Conf. Curves and Surfaces*, Chamonix, France, 1996.
8. T. Darrell and A. Pentland. Cooperative robust estimation using layers of support. *IEEE Trans. Patt. Anal. and Mach. Int.*, 17(5):474–487, 1995.
9. X. Descombes and F. Kruggel. A markov pixion information approach for low-level image description. *IEEE Trans. Patt. Anal. and Mach. Int.*, 21(6):482–494, 1999.
10. S. Geman and D. Geman. Stochastic relaxation, gibbs distributions, and the bayesian restoration of images. *IEEE Trans. Patt. Anal. and Mach. Int.*, 6(6):721–741, 1984.
11. J. Istas. *Statistics of processes and signal-image segmentation*. University of Paris VII, 1997.
12. I. Jermyn and H. Ishikawa. Globally optimal regions and boundaries. In *Int. Conf. on Comp. Vis.*, pages 904–910, Kerkyra, Greece, September 1999.
13. M. Kass, A. Witkin, and D. Terzopoulos. Snakes: active contour models. *Int J. Computer Vision*, 12(1):321–331, 1987.
14. C. Kervrann, M. Hoebeke, and A. Trubuil. A level line selection approach for object boundary estimation. In *Int. Conf. on Comp. Vis.*, pages 963–968, Kerkyra, Greece, September 1999.
15. Y. Leclerc. Constructing simple stable descriptions for image partitioning. *Int J. Computer Vision*, 3:73–102, 1989.
16. G. Matheron. *Random Sets and Integral Geometry*. John Wiley, New York, 1975.
17. J. Møller and R. Waagepetersen. Markov connected component fields. *Adv. in Applied Probability*, pages 1–35, 1998.
18. P. Monasse and F. Guichard. Scale-space from a level line tree. In *Int. Conf. on Scale-Space Theories Comp. Vis.*, pages 175–186, Kerkyra, Greece, September 1999.
19. J. Morel and S. Solimini. *Variational Methods in Image Segmentation*. Birkhauser, 1994.
20. D. Mumford. The Bayesian rationale for energy functionals. *Geometry-Driven Diffusion in Computer Vision*, pages 141–153, Bart Romeny ed., Kluwer Academic, 1994.
21. D. Mumford and J. Shah. Optimal approximations by piecewise smooth functions and variational problems. *Communication on Pure and applied Mathematics*, 42(5):577–685, 1989.
22. S. Osher and J. Sethian. Fronts propagating with curvature dependent speed: algorithms based on the hamilton-jacobi formulation. *J. Computational Physics*, 79:12–49, 1988.

23. F. O'Sullivan and M. Qian. A regularized contrast statistic for object boundary estimation – implementation and statistical evaluation. *IEEE Trans. Patt. Anal. and Mach. Int.*, 16(6):561–570, 1994.
24. N. Paragios and R. Deriche. Coupled geodesic active regions for image segmentation: a level set approach. In *Euro. Conf. on Comp. Vis.*, Dublin, Ireland, 2000.
25. T. Pavlidis and Y. Liow. Integrating region growing and edge detection. *IEEE Trans. Patt. Anal. and Mach. Int.*, 12:225–233, 1990.
26. C. Schnörr. A study of a convex variational diffusion approach for image segmentation and feature extraction. *J. Math. Imaging and Vision*, 3(8):271–292, 1998.
27. J. Wang. Stochastic relaxation on partitions with connected components and its application to image segmentation. *IEEE Trans. Patt. Anal. and Mach. Int.*, 20(6):619–636, 1998.
28. L. Younes. Calibrating parameters of cost functionals. In *Euro. Conf. on Comp. Vis.*, Dublin, Ireland, 2000.
29. S. Zhu and A. Yuille. Region competition: unifying snakes, region growing, and bayes/MDL for multiband image segmentation. *IEEE Trans. Patt. Anal. and Mach. Int.*, 18(9):884–900, 1996.